Bulletin of Electrical Engineering and Informatics
Vol. 15, No. 6, December 2026, pp. 4924~4934
ISSN: 2302-9285, DOI: 10.11591/eei.v15i6.11622

Wearable antenna for non-invasive human arm bone fracture monitoring system

Mohd Saiful Riza Bashri[1], Noor Amalina Ramli[2], Abang Muhammad Sufi Abang Madehan[3]
[1]Department of Science in Engineering, Kulliyyah of Engineering, International Islamic University Malaysia, Kuala Lumpur, Malaysia
[2]Department of Electrical and Electronic Engineering, Faculty of Engineering, Universiti Pertahanan Nasional Malaysia, Kuala Lumpur, Malaysia
[3]Department of Electrical and Computer Engineering, Kulliyyah of Engineering, International Islamic University Malaysia, Kuala Lumpur, Malaysia

Article Info

Article history:

Received Oct 14, 2025
Revised Sep 9, 2026
Accepted Sep 12, 2026

Keywords:

Biomedical application
Bone monitoring
Microwave sensing
Monopole antenna
Wearable antenna

ABSTRACT

This paper presents a flexible wearable monopole antenna for non-invasive monitoring of human arm bone fracture healing. The antenna is fabricated on a polyethylene terephthalate (PET) substrate and is intended for integration into an arm cast for continuous monitoring during healing. With dimensions of 77 mm×53 mm×0.2 mm, the antenna operates from 1.7 to 2.6 GHz in free space and exhibits resonance changes when placed on a human arm phantom. Bone healing is assessed through changes in the antenna reflection coefficient caused by variations in the dielectric properties around the fracture site. Experimental measurements show resonance at approximately 1.84 GHz without blood, 1.88 GHz with 10 ml of blood, and 1.82 GHz with 20 ml of blood, demonstrating sensitivity to changes associated with the healing process. The simulated specific absorption rate is 0.0452 W/kg at 1 mW transmitted power, within accepted safety limits. The agreement between simulation and measurement supports the feasibility of the proposed compact, low-cost, and non-invasive monitoring approach.

This is an open access article under the CC BY-SA license.

Corresponding Author:

Noor Amalina Ramli
Department of Electrical and Electronic Engineering, Faculty of Engineering
Universiti Pertahanan Nasional Malaysia
57000 Kem Sungai Besi, Kuala Lumpur, Malaysia
Email: nooramalina@upnm.edu.my

1. INTRODUCTION

Microwave technology has gained significant attention in recent years for biomedical diagnostic applications, particularly in imaging and wearable sensing systems. Several studies have investigated microwave-based approaches for head imaging, including the development of body-coupled and wearable antennas for diagnostic purposes [1]–[4]. For example, Sakib *et al*. [1] proposed a barium titanate-silicon elastomer-based body-coupled antenna for wearable microwave head imaging, while Rodriguez-Duarte *et al*. [3] and Alqadami *et al*. [4] earlier works, focused on wearable devices and flexible antenna arrays for head diagnostic systems. Tømmer *et al*. [2] also demonstrated a body-coupled wideband monopole antenna, highlighting the relevance of body-conformal antenna structures in biomedical applications. In addition, flexible and polymer-based antenna arrays have been reported for brain stroke diagnosis, showing the potential of wearable microwave systems for safe and portable monitoring [5], [6]. Beyond medical head imaging, microwave-based sensing has also been investigated for other biomedical applications, including breast cancer detection [7], urinary bladder volume and state monitoring [8], [9], non-invasive glucose monitoring [10], hydration assessment [11], brain stroke monitoring [12], skin cancer detection [13], and

lung tumor detection [14]. These studies further demonstrate the potential of microwave techniques for detecting physiological and pathological changes through variations in the dielectric properties of biological tissues.

Several studies have explored microwave sensing for bone fracture monitoring, but most were not developed for wearable use. Hossen *et al.* [15] presented a double-negative (DNG) metamaterial-inspired slotted Vivaldi antenna integrated with supervised machine learning for ex-vivo bone fracture diagnosis. Although promising, the system was developed as a diagnostic setup rather than a wearable monitoring device. Santos *et al*. [16] investigated the feasibility of microwave imaging for bone fracture detection, demonstrating the potential of imaging-based analysis, but the approach was not intended for continuous wearable monitoring. Ramalingam *et al*. [17] developed a compact microwave device for diagnosing tibia fractures; however, it was designed as a standalone diagnostic instrument rather than a body-integrated sensor. Moqadam and Kazemi [18] proposed a dual-polarized microwave sensor based on reactive impedance surfaces for bone fracture detection, but the reported configuration was not aimed at wearable implementation. Boologam *et al.* [19] studied a planar monopole antenna for bone crack and void detection, focusing mainly on sensing capability rather than long-term body-worn use. In contrast, Symeonidis *et al.* [20] investigated implanted antennas for fracture monitoring in heterogeneous bone phantoms, which makes the approach invasive. Riaz *et al.* [21] reported a non-invasive ultra high frequency (UHF) antenna-based method for bone fracture monitoring, but the work did not focus on a wearable cast-integrated structure. Similarly, Kiris *et al*. [22] examined the use of a helical antenna as a bone fracture sensor, yet the design was not presented as a flexible or wearable solution. These limitations highlight the need for a non-invasive, flexible, and patient-friendly wearable system for continuous bone healing assessment. A compact textile monopole antenna for bone healing monitoring was reported in [23], but its higher operating frequency may reduce its suitability for sensing fractures located deeper within muscle tissue. These limitations indicate a clear need for a safe, flexible, low-profile, and patient-friendly wearable system for continuous bone healing assessment.

Therefore, this work proposes a microwave-based wearable antenna integrated into a cast as a promising approach for non-invasive and practical clinical monitoring. Figure 1 illustrates the progression of fractured-bone healing from the initial inflammatory stage through callus formation and bone remodeling [24].

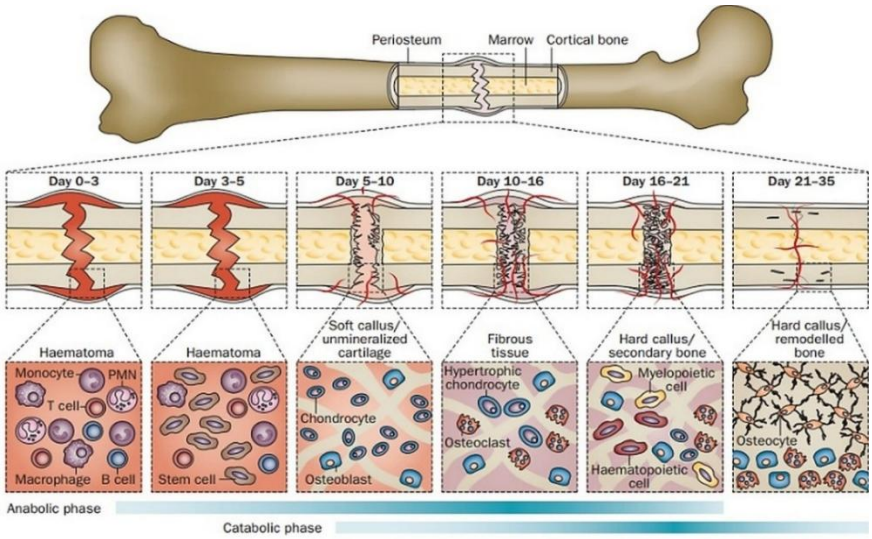


Figure 1. Healing process of fractured bone [24]

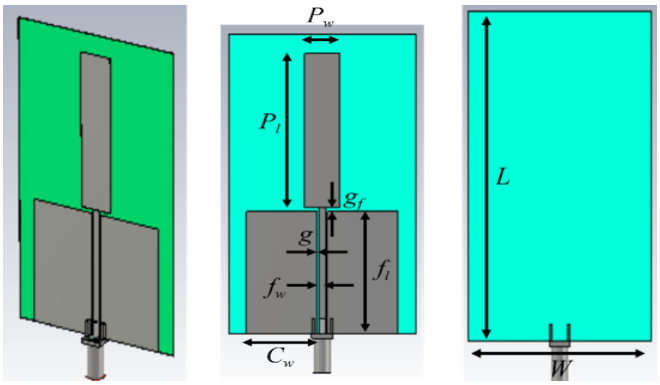
2. METHODS

2.1. Antenna design

A rectangular planar monopole antenna was designed to operate at 2 GHz as shown in Figure 2. Figure 2(a) presents the three-dimensional antenna configuration, Figure 2(b) shows the top view and principal dimensions, and Figure 2(c) shows the bottom view. The antenna is fully planar and does not require a separate ground plane, as it employs a coplanar waveguide (CPW) structure as the feeding line. The initial length of the rectangular monopole antenna was calculated using (1):

$$L = 0.25 \times \lambda_g \quad (1)$$

where the guided wavelength, $\lambda_g = 1/\sqrt{\varepsilon_r}$. The dielectric constant of the substrate, ε_r is 2.3. The feeding line is made of coplanar waveguide (CPW) structure where its characteristic impedance is 50 Ω.



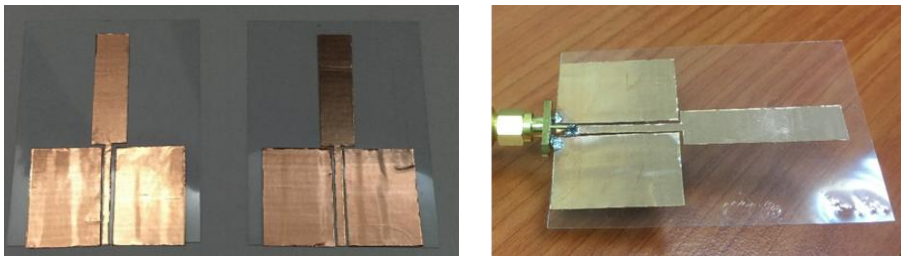
(a) (b) (c)

Figure 2. Geometry of the proposed wearable monopole antenna: (a) 3D view, (b) top view, and (c) bottom view

The antenna is fabricated on a flexible polyethylene terephthalate (PET) substrate with a thickness of 0.2 mm and a loss tangent of 0.003. PET was chosen due to its mechanical flexibility, thin profile, dimensional stability, ease of fabrication, and relatively low dielectric loss, which make it well suited for integration into a cast structure. In comparison with textile-based materials, PET also offers more stable geometry and reduced performance variation due to moisture absorption. The finalized design parameters are listed in Table 1. The flexibility of the substrate makes it well-suited for wearable applications. The antenna was then fabricated using copper tape as the conducting structure as shown in Figure 3. Figure 3(a) shows the fabricated antenna from the top, while Figure 3(b) shows the antenna connected to the SMA connector for measurement.

Table 1. The physical dimension of the proposed antenna

Parameter	Symbol	Value (mm)
Substrate length	L	77
Substrate width	W	53
Patch length	P_l	39.5
Patch width	P_w	10
Feed line length	f_l	32.5
Feed line width	f_w	2
CPW width	C_w	20
Gap	g	0.5
Feed line gap	g_f	1



(a) (b)

Figure 3. Fabricated proposed wearable antenna: (a) top view and (b) antenna connected to the SMA connector

2.2. Human arm phantom

2.2.1. Phantom design in simulation

A three-layer human arm phantom was modeled in computer simulation technology (CST) as a coaxial cylinder consisting of bone marrow, cortical bone, and muscle using the dimensions shown in Table 2. The electrical properties of each layer were taken from [25] as shown in Table 3. Although the

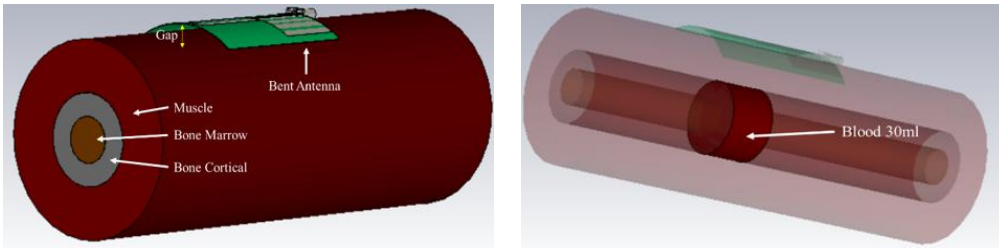
dimensions were originally based on the femur, the model is valid for the arm since the dielectric properties of marrow, cortical bone, and muscle are consistent across human limbs. For proof-of-concept, a single bone was modeled with a marrow–cortical diameter of 40 mm and a surrounding muscle thickness of 22.5 mm. All layers were concentric, and the phantom length was chosen to fully enclose the antenna geometry. The 3D model of the human arm phantom in the simulation attached to the proposed antenna is illustrated in Figure 4. Figure 4(a) shows the proposed antenna positioned on the simulated human arm phantom, while Figure 4(b) provides a transparent view of the phantom and the blood region surrounding the fractured bone.

Table 2. Dimensions of human arm phantom

Layer	Radius (mm)	Length (mm)
Bone marrow	10	230
Bone cortical	20	230
Muscle	42.5	230
Blood 10 ml	20	8
Blood 30 ml	20	24

Table 3. Parameters of human arm phantom

Tissue	Dielectric constant (ε)	Conductivity (S/m)	Frequency (GHz)
Bone marrow	5.2644	0.10877	2.75
Bone cortical	11.207	0.45429	2.75
Muscle	52.363	1.9515	2.75
Blood	60.12	17.01	2.40



(a) (b)

Figure 4. Simulated human arm phantom and antenna configuration: (a) antenna on the human arm model and (b) transparent view showing blood around the fractured bone

2.2.2. Fabricated human arm phantom

To validate the simulation, a realistic three-layer arm phantom was fabricated using household materials as listed in Table 4. The phantom was designed to replicate the dielectric properties of bone marrow, cortical bone, and muscle in the 0.5–4 GHz frequency range. Anatomical phantoms made from household materials are preferred over ex vivo tissue for microwave measurements due to their hygienic nature, low cost, and suitability for long-term experiments, as they do not spoil actual human or animal tissue.

Table 4. Ingredients for human arm phantom

Ingredient	Bone marrow	Bone cortical	Muscle	Blood
Flour (g)	80	80	-	-
Sugar (g)	-	7.2	-	45.5
Salt (g)	-	-	-	0.5
Deionised water (ml)	3	10.5	800	82.5
Gelatine (g)	-	-	100	-
Detergent (ml)	-	-	-	-
Oil (ml)	33	30	31	-
Food colouring (ml)	1	-	-	0.5

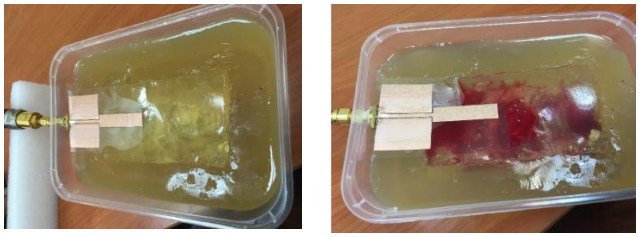
Figure 5 illustrates the fabricated human arm phantom employed in the experimental validation of the proposed bone healing monitoring system using a wearable microwave sensing technique. Figure 5(a) shows the fabricated marrow and cortical-bone layers, Figure 5(b) shows the opening in the muscle phantom, Figure 5(c) shows the bone positioned inside the muscle phantom, and Figure 5(d) shows the completed layered phantom.



(a) (b) (c) (d)

Figure 5. Fabrication stages of the human arm phantom: (a) bone marrow inside the cortical bone, (b) cut inside the muscle phantom, (c) bone placed inside the muscle phantom, and (d) bone layer covered by the muscle layer

Figure 6 shows the experimental setup used to validate the performance of the proposed wearable antenna for monitoring bone healing with the artificial human arm phantom. The antenna was placed directly on top of the muscle layer of the phantom. Different volumes of artificial blood were injected into the bone phantom, and the antenna's reflection coefficient was measured. Figure 6(a) shows the antenna placed on the fabricated arm phantom before blood injection, while Figure 6(b) shows the phantom after artificial blood was injected into the bone region.



(a) (b)

Figure 6. Experimental human arm phantom setup: (a) antenna placement on the phantom without blood and (b) phantom injected with blood

3. RESULTS AND DISCUSSION

This section presents and discusses the simulation and experimental results of the proposed flexible monopole antenna for bone healing monitoring.

3.1. Simulation

The reflection coefficient of the antenna when simulated in free space without the presence of the human arm phantom shows operating frequency bandwidth from 1.7 GHz to 2.6 GHz as shown in Figure 7. The operating frequency range was chosen to ensure the electromagnetic wave can penetrate deep inside the human arm to probe the bone. Moreover, it also makes it possible to design a compact wearable antenna where the intention is to be embedded inside the casting of the broken arm.

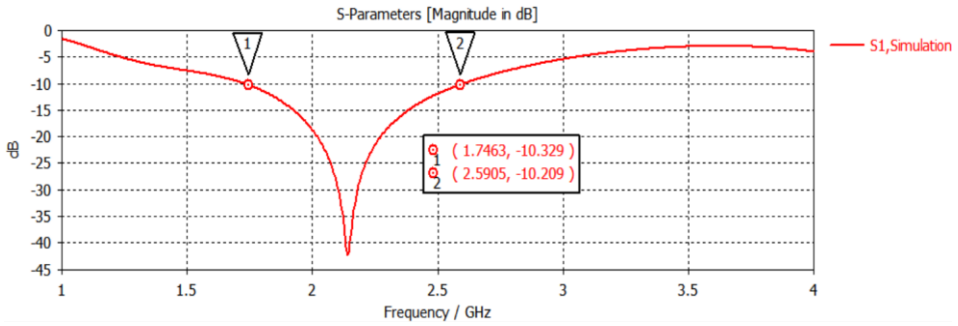


Figure 7. Simulated reflection coefficient of the antenna in free space

Figure 8 shows the 3D radiation pattern of the antenna in free space, which exhibits the typical omnidirectional characteristics of a monopole antenna. The simulated gain is 2.7 dBi. The operating frequency bandwidth of the antenna shifted from 1.7–2.6 GHz in free space to 2.2–3.0 GHz when placed on the human arm phantom, indicating a 400 MHz upward shift as shown in Figure 9. Nevertheless, the antenna still covers the intended frequency range; therefore, no further modification of the antenna parameters was required.

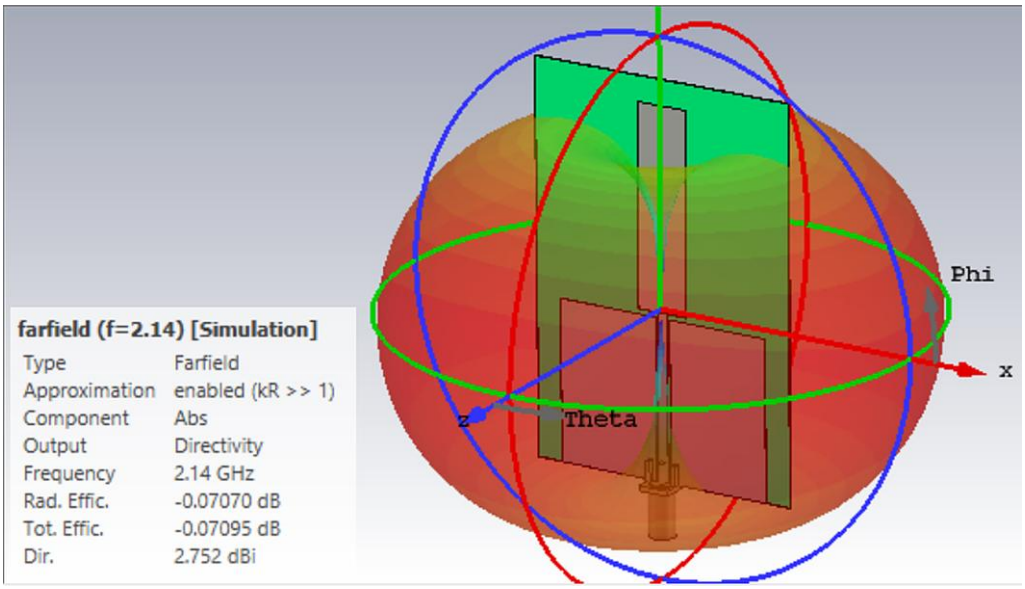


Figure 8. Simulated 3D radiation pattern of the antenna in free space

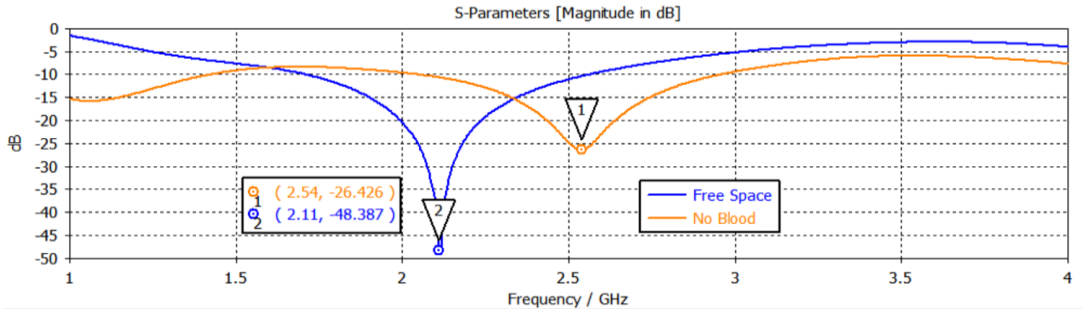
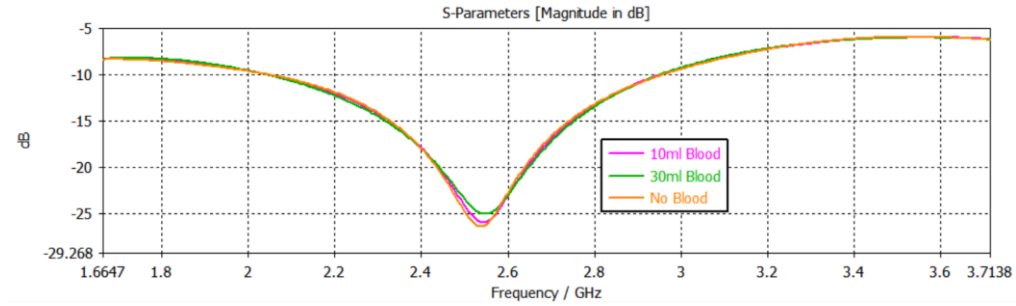


Figure 9. Simulated reflection coefficient with the presence of human arm phantom

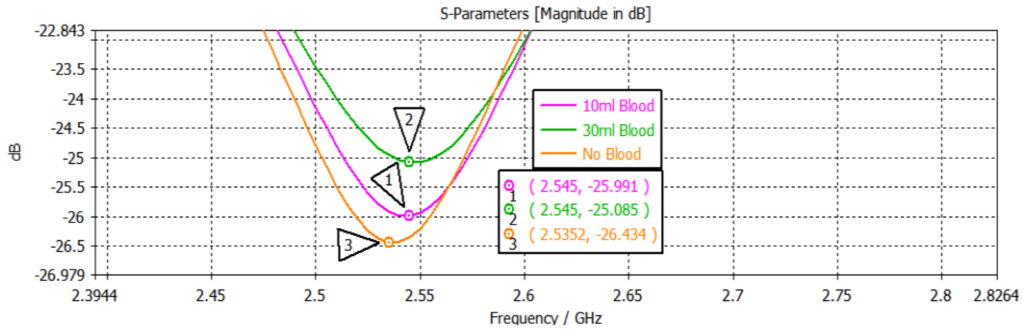
Figure 10 shows the simulated reflection coefficient of the antenna for different blood volumes ranging from 10 ml to 30 ml. A clear shift in the reflection coefficient can be observed as the injected blood volume increases. Figure 10(a) compares the simulated reflection coefficients for the no-blood, 10 ml, and 30 ml blood cases, while Figure 10(b) enlarges the resonance region to show the frequency shifts more clearly.

3.2. Experiment

Figure 11 compares the reflection coefficient of the proposed antenna in free space and when placed on the human arm phantom. In free space, the antenna resonates around 2.45 GHz with a return loss of approximately –25 dB, providing a bandwidth centered within the intended operating frequency. When positioned on the phantom, the resonance shifts downward to about 1.9 GHz, corresponding to a frequency shift of nearly 500 MHz. This detuning occurs because the high permittivity and conductive properties of biological tissue increase the effective electrical length of the antenna, lowering its resonant frequency. Although the resonance shifts, the antenna maintains sufficient impedance matching within the frequency range of interest, confirming its potential for bone healing monitoring in realistic conditions.



(a)



(b)

Figure 10. Simulated reflection-coefficient response for different blood volumes: (a) no blood, 10 ml, and 30 ml cases and (b) zoomed-in view of the resonance region

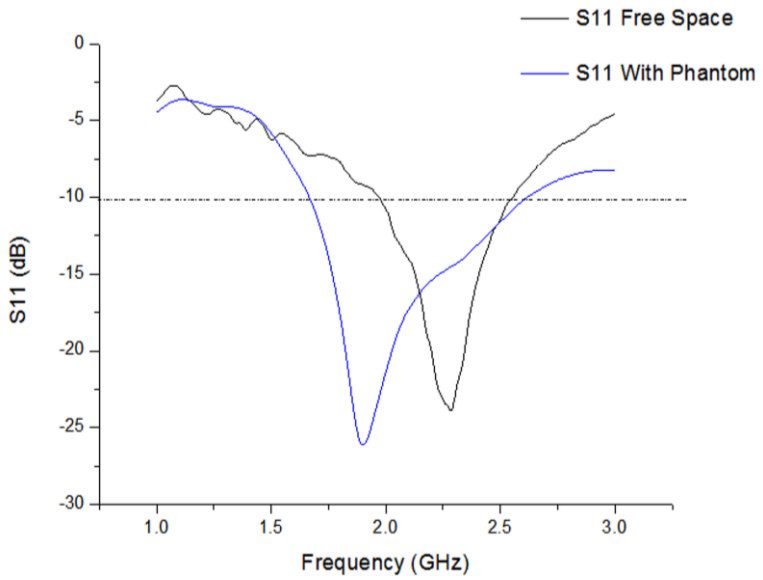


Figure 11. Measured reflection coefficient in free space and with the human arm phantom

Figure 12 presents the measured reflection coefficients of the antenna with different blood volumes injected into the bone phantom. In the no-blood case, the antenna resonates at approximately 1.84 GHz with good impedance matching. With the addition of 10 ml of blood, the resonance shifts upward to about 1.88 GHz, while for 20 ml of blood, the resonance moves downward to around 1.82 GHz. These shifts confirm that the antenna's resonant frequency is influenced by the presence and amount of blood, as changes in blood volume modify the dielectric properties around the bone region. The measured results are consistent with the simulation findings, showing a similar trend in frequency shifts. This agreement validates the accuracy of the simulation model and further demonstrates the antenna's potential for detecting physiological changes relevant to bone healing monitoring.

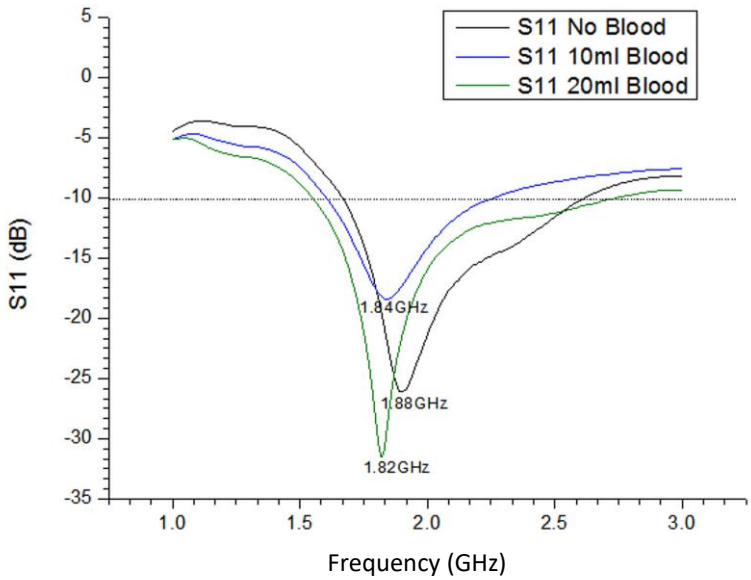


Figure 12. Measured reflection coefficients with no blood, 10 ml, and 20 ml of blood

In general, lower frequencies are more favorable for deeper tissue penetration, but they require larger antenna dimensions, which may reduce suitability for wearable integration. In contrast, higher frequencies allow more compact antenna designs and may offer finer spatial sensitivity, but they are generally less suitable for interrogating deeper tissue regions. Therefore, the chosen operating band represents a practical compromise between sensing depth and wearable form factor. In addition, the simulated specific absorption rate (SAR) of the proposed system was found to be 0.0452 W/kg for 1 mW transmitted power as shown in Figure 13, which remains within commonly accepted international safety limits for localized exposure. This indicates that the antenna configuration is suitable for wearable biomedical sensing applications while maintaining safe electromagnetic exposure levels.

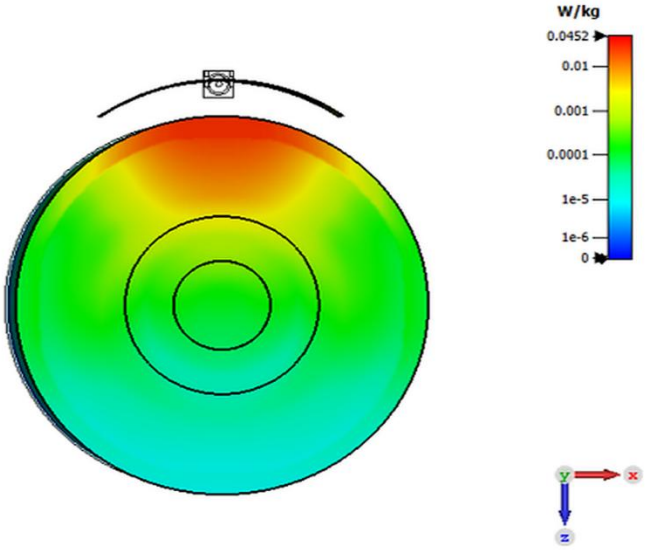


Figure 13. Simulated SAR distribution on the human arm phantom

Since the present study is limited to controlled phantom-based proof-of-concept testing, several practical factors that may arise in real clinical use have not yet been fully investigated. Patient movement, sweat, imperfect contact between the antenna and the cast surface, variations in cast thickness, and inter-patient anatomical differences may influence the antenna's impedance matching and resonance behavior. These effects could introduce additional variability in the measured response under real-world conditions. Therefore, although the current results demonstrate the feasibility of the proposed approach,

dedicated future studies are required to systematically evaluate these factors before practical deployment can be considered. A comparison between the proposed system and previously reported microwave-based bone monitoring techniques is summarized in Table 5, highlighting the advantages of the proposed wearable and non-invasive approach for continuous bone healing assessment.

Table 5. Comparison of existing microwave-based bone monitoring systems with the proposed work

Ref.	Method/antenna type	Wearable	Non-invasive	Operating frequency	Bone monitoring capability	Main limitation
Hossen *et al*. [15]	DNG metamaterial-inspired slotted Vivaldi antenna with machine learning.	No	Yes	Microwave band	Ex-vivo bone fracture diagnosis	Not designed for continuous wearable monitoring.
Santos *et al*. [16]	Microwave imaging system.	No	Yes	Microwave band	Bone fracture detection	Imaging setup not suitable for wearable use.
Ramalingam *et al*. [17]	Compact microwave diagnostic device.	No	Yes	Microwave band	Tibia fracture diagnosis	Standalone diagnostic instrument.
Moqadam and Kazemi [18]	Dual-polarized microwave sensor with reactive impedance surface.	No	Yes	Microwave band	Bone fracture detection	Not intended for flexible wearable integration.
Boologam *et al*. [19]	Planar monopole antenna.	No	Yes	Microwave band	Bone crack and void detection	Focused mainly on sensing performance.
Symeonidis *et al*. [20]	Implanted antenna sensor.	No	No (invasive)	Microwave band	Fracture monitoring	Requires implantation.
Riaz *et al*. [21]	UHF antenna-based monitoring system.	Partial	Yes	UHF band	Bone fracture monitoring	Did not focus on cast-integrated wearable structure.
Kiris *et al*. [22]	Helical antenna sensor.	No	Yes	Microwave band	Bone fracture sensing	Not flexible or wearable.
Rizwan *et al*. [23]	Textile monopole antenna with machine learning.	Yes	Yes	Higher frequency band	Bone healing monitoring	Higher frequency may reduce deep tissue penetration.
This work	Flexible CPW-fed wearable monopole antenna integrated into cast.	Yes	Yes	1.7–2.6 GHz	Continuous bone healing monitoring through dielectric variation	Phantom-based proof-of-concept validation.

4. CONCLUSION

A wearable antenna for bone healing monitoring has been successfully designed, simulated, and experimentally validated. The antenna, intended to be integrated into an arm cast, enables continuous and non-invasive monitoring of the fracture healing process during the critical early stages. Both simulation and measurement results demonstrated that the reflection coefficient of the antenna is sensitive to variations in the dielectric properties of the bone, particularly changes in blood content around the fracture site. The observed frequency shifts with different blood volumes confirm the antenna's ability to detect physiological changes associated with bone healing. The consistency between simulation and experimental findings further validates the proposed design. Unlike conventional monitoring methods such as X-ray and computed tomography (CT), which are not suitable for safe, repeated, and continuous monitoring due to radiation exposure, the proposed approach offers a radiation-free and potentially wearable alternative. Overall, the study shows that the developed wearable antenna offers a promising solution for real-time bone healing assessment, potentially improving patient care and clinical decision-making.

FUNDING INFORMATION

The research work was supported by Ministry of Higher Education of Malaysia under the Fundamental Research Grant Scheme FRGS21-246-0855 (Grant no. FRGS/1/2021/TK0/UIAM/02/25).

AUTHOR CONTRIBUTIONS STATEMENT

This journal uses the Contributor Roles Taxonomy (CRediT) to recognize individual author contributions, reduce authorship disputes, and facilitate collaboration.

Name of Author	C	M	So	Va	Fo	I	R	D	O	E	Vi	Su	P	Fu
Mohd Saiful Riza Bashri	✓	✓	✓	✓	✓	✓	✓	✓	✓	✓		✓	✓	
Noor Amalina Ramli			✓		✓			✓	✓	✓	✓	✓		
Abang Muhammad Sufi Abang Madehan	✓	✓	✓	✓		✓	✓			✓	✓		✓	

C : **C**onceptualization
M : **M**ethodology
So : **So**ftware
Va : **Va**lidation
Fo : **Fo**rmal analysis
I : **I**nvestigation
R : **R**esources
D : **D**ata Curation
O : Writing - **O**riginal Draft
E : Writing - Review & **E**diting
Vi : **Vi**sualization
Su : **Su**pervision
P : **P**roject administration
Fu : **Fu**nding acquisition

CONFLICT OF INTEREST STATEMENT

Authors state no conflict of interest.

DATA AVAILABILITY

Data availability is not applicable to this paper as no new data were created or analyzed in this study.

REFERENCES

[1] M. A. T. Sakib, M. S. R. Bashri, and M. R. Islam, "Barium titanate–silicon elastomer based body coupled antenna for wearable microwave head imaging applications," *Bulletin of Electrical Engineering and Informatics (BEEI)*, vol. 13, no. 3, pp. 1566–1573, Jun. 2024, doi: 10.11591/eei.v13i3.6665.

[2] M. Tømmer, K. G. Kjelgård, and T. S. Lande, "Body coupled wideband monopole antenna," in *2016 Loughborough Antennas and Propagation Conference, LAPC 2016*, Nov. 2017, pp. 1–5, doi: 10.1109/LAPC.2016.7807483.

[3] D. O. Rodriguez-Duarte, C. Origlia, J. A. T. Vasquez, R. Scapaticci, L. Crocco, and F. Vipiana, "Wearable Microwave Imaging System for Brain Stroke Imaging," in *2022 IEEE International Symposium on Antennas and Propagation and USNC-URSI Radio Science Meeting (AP-S/USNC-URSI)*, 2022, pp. 1716–1717, doi: 10.1109/AP-S/USNC-URSI47032.2022.9887338.

[4] A. S. M. Alqadami, A. E. Stancombe, K. S. Bialkowski, and A. Abbosh, "Flexible Meander-Line Antenna Array for Wearable Electromagnetic Head Imaging," *IEEE Transactions on Antennas and Propagation*, vol. 69, no. 7, pp. 4206–4211, Jul. 2021, doi: 10.1109/TAP.2020.3037742.

[5] A. S. M. Alqadami, K. S. Bialkowski, A. T. Mobashsher, and A. M. Abbosh, "Wearable Electromagnetic Head Imaging System Using Flexible Wideband Antenna Array Based on Polymer Technology for Brain Stroke Diagnosis," *IEEE Transactions on Biomedical Circuits and Systems*, vol. 13, no. 1, pp. 124–134, Feb. 2019, doi: 10.1109/TBCAS.2018.2878057.

[6] B. J. Mohammed, A. M. Abbosh, S. Mustafa, and D. Ireland, "Microwave system for head imaging," *IEEE Transactions on Instrumentation and Measurement*, vol. 63, no. 1, pp. 117–123, Jan. 2014, doi: 10.1109/TIM.2013.2277562.

[7] M. T. Islam, M. Z. Mahmud, M. T. Islam, S. Kibria, and M. Samsuzzaman, "A Low Cost and Portable Microwave Imaging System for Breast Tumor Detection Using UWB Directional Antenna array," *Scientific Reports*, vol. 9, no. 1, p. 15491, Oct. 2019, doi: 10.1038/s41598-019-51620-z.

[8] S. A. Samad, T. Arslan, S. Saher, and I. Saied, "Urinary Bladder Volume Monitoring System With Antenna Array-Based Flexible Sensor," *IEEE Sensors Journal*, vol. 25, no. 11, pp. 20333–20341, Jun. 2025, doi: 10.1109/JSEN.2025.3556631.

[9] A. Farshkaran, A. Fry, A. Raterink, A. Santorelli, and E. Porter, "Proof-of-Concept of Microwave-Based Bladder State Detection Using Realistic Pelvic Models," *IEEE Open Journal of Engineering in Medicine and Biology*, vol. 5, pp. 140–147, 2024, doi: 10.1109/OJEMB.2023.3305838.

[10] Y. Zaarour *et al*., "Microwave Antenna Sensing for Glucose Monitoring in a Vein Model Mimicking Human Physiology," *Biosensors*, vol. 15, no. 5, p. 282, Apr. 2025, doi: 10.3390/bios15050282.

[11] D. Agarwal *et al.*, "A Non-Invasive Hydration Monitoring Technique Using Microwave Transmission and Data-Driven Approaches," *Sensors*, vol. 22, no. 7, p. 2536, Mar. 2022, doi: 10.3390/s22072536.

[12] A. Cuccaro, A. Dell'Aversano, B. Basile, M. A. Maisto, and R. Solimene, "Subcranial Encephalic Temnograph-Shaped Helmet for Brain Stroke Monitoring," *Sensors*, vol. 24, no. 9, p. 2887, Apr. 2024, doi: 10.3390/s24092887.

[13] K. Kaur and A. Kaur, "In vitro detection of skin cancer using an UWB stacked micro strip patch antenna with microwave imaging," *International Journal of RF and Microwave Computer-Aided Engineering*, vol. 32, no. 12, e23407, 2022, doi: 10.1002/mmce.23407.

[14] W. Alamro, B.-C. Seet, L. Wang, and P. Parthiban, "Early-Stage Lung Tumor Detection Based on Super-Wideband Microwave Reflectometry," *Electronics*, vol. 12, no. 1, p. 36, 2023, doi: 10.3390/electronics12010036.

[15] M. S. Hossen, A. Hoque, M. T. Islam, P. Kirawanich, M. H. Baharuddin, and M. S. Soliman, "DNG metamaterial-inspired slotted Vivaldi antenna development integrated with supervised machine learning for ex-vivo bone fracture diagnosis," *Ain Shams Engineering Journal*, vol. 16, no. 8, p. 103464, Aug. 2025, doi: 10.1016/j.asej.2025.103464.

[16] K. C. Santos, C. A. Fernandes, and J. R. Costa, "Feasibility of Bone Fracture Detection Using Microwave Imaging," *IEEE Open Journal of Antennas and Propagation*, vol. 3, pp. 836–847, 2022, doi: 10.1109/OJAP.2022.3194217.
[17] V. S. Ramalingam, M. Kanagasabai, and E. F. Sundarsingh, "A Compact Microwave Device for Fracture Diagnosis of the Human Tibia," *IEEE Transactions on Components, Packaging and Manufacturing Technology*, vol. 9, no. 4, pp. 661–668, Apr. 2019, doi: 10.1109/TCPMT.2019.2893367.
[18] A. N. Moqadam and R. Kazemi, "Design of a novel dual-polarized microwave sensor for human bone fracture detection using reactive impedance surfaces," *Scientific Reports*, vol. 13, no. 1, p. 10776, Jul. 2023, doi: 10.1038/s41598-023-38039-3.
[19] A. V. Boologam *et al.*, "On the Design and Development of Planar Monopole Antenna for Bone Crack/Void Detection," *International Journal of Antennas and Propagation*, vol. 2022, pp. 1–12, May 2022, doi: 10.1155/2022/4663488.
[20] S. Symeonidis, W. G. Whittow, M. Zecca, and C. Panagamuwa, "Bone fracture monitoring using implanted antennas in the radius, tibia and phalange heterogeneous bone phantoms," *Biomedical Physics and Engineering Express*, vol. 4, no. 4, 2018, doi: 10.1088/2057-1976/aab974.
[21] M. Riaz, G. Tiberi, H. Asani, M. Ghavami, and S. Dudley, "A Non-Invasive Bone Fracture Monitoring Analysis using an UHF Antenna," in *2020 12th International Symposium on Communication Systems, Networks and Digital Signal Processing, CSNDSP 2020*, Jul. 2020, pp. 1–5, doi: 10.1109/CSNDSP49049.2020.9249570.
[22] S. Kiris, A. Incesu, M. Karaaslan, O. Akgol, and E. Unal, "Study of Helical Antenna as a Bone Fracture Sensor," in *4th International Symposium on Multidisciplinary Studies and Innovative Technologies, ISMSIT 2020 - Proceedings*, Oct. 2020, pp. 1–4, doi: 10.1109/ISMSIT50672.2020.9254610.
[23] S. Rizwan, K. V. P. Kumar, and A. J. Alazemi, "A Compact Textile Monopole Antenna for Monitoring the Healing of Bone Fractures Using Un-Supervised Machine Learning Algorithm," *IEEE Access*, vol. 11, pp. 101195–101204, 2023, doi: 10.1109/ACCESS.2023.3314577.
[24] T. A. Einhorn and L. C. Gerstenfeld, "Fracture healing: Mechanisms and interventions," *Nature Reviews Rheumatology*, vol. 11, no. 1, pp. 45–54, Jan. 2015, doi: 10.1038/nrrheum.2014.164.
[25] G. Ruvio, A. Cuccaro, R. Solimene, A. Brancaccio, B. Basile, and M. J. Ammann, "Microwave bone imaging: A preliminary scanning system for proof-of-concept," *Healthcare Technology Letters*, vol. 3, no. 3, pp. 218–221, Sep. 2016, doi: 10.1049/htl.2016.0003.

BIOGRAPHIES OF AUTHORS



Mohd Saiful Riza Bashri received the bachelor degree in Communication Engineering and master of science in Electronics Engineering from International Islamic University Malaysia (IIUM) in 2009 and 2014 respectively. He obtained his Ph.D. degree in Engineering from the University of Edinburgh, Scotland in 2018. Currently, he is an assistant professor with the Department of Science in Engineering, Kulliyyah of Engineering, IIUM. His research interests include antenna design, microwave-based biomedical imaging, RFID, and biosensors. He can be contacted at email: mohdsaifulriza@iium.edu.my.



Noor Amalina Ramli received the bachelor's degree in Communication Engineering and the Master of Science degree in Electronics from the International Islamic University Malaysia (IIUM) in 2009 and 2012, respectively. She obtained her Ph.D. degree in Engineering from the University of Edinburgh, Scotland in 2018. She is currently a lecturer with the Faculty of Engineering, Universiti Pertahanan Nasional Malaysia (UPNM). Prior to joining UPNM, she worked as an application engineer at CAD-IT Consultants, specializing in simulation solutions for electronics and multiphysics applications. Her research interests include RF and microwave devices, antenna design, electromagnetic simulation, MEMS, advanced packaging, and sensors. She can be contacted at email: nooramalina@upnm.edu.my.



Abang Muhammad Sufi Abang Madehan received the bachelor degree in communication engineering from International Islamic University Malaysia (IIUM) in 2020. Currently, he is pursuing his master degree with the Department of Electrical and Computer, Kulliyyah of Engineering, IIUM. His research interests include antenna design, microwave-based biomedical imaging and artificial intelligence on 5G applications. He can be contacted at email: abang.sufi@live.iium.edu.my.